SME Annual Meeting
Feb. 25 - 28, 2018, Minneapolis, MN

Preprint 18-050

INFLUENCE OF A CONTINUOUS MINING MACHINE AND ROOF/RIB MESH ON MAGNETIC PROXIMITY DETECTION SYSTEMS

J. Li, NIOSH, Pittsburgh, PA
C. Zhou, NIOSH, Pittsburgh, PA
J. H. DuCarme, NIOSH, Pittsburgh, PA
C. C. Jobes, NIOSH, Pittsburgh, PA

ABSTRACT

Magnetic proximity detection systems (PDSs) are used with continuous mining machines (CMMs) to protect miners from striking and pinning accidents. Generators are used in a PDS to create magnetic fields covering the space around a CMM. The PDS determines the proximity of a miner relative to the CMM based on the magnetic flux density detected by a miner-wearable component (MWC) and simultaneously alerts the miner and stops the motion of the CMM if the miner is within a proximity that creates a striking hazard. A stable magnetic field is essential to the accuracy of the proximity calculations performed by the PDS. This paper presents the results of a systematic study of the magnetic influence of two types of steel structures found near a CMM—the body of the CMM itself and the wire mesh used for roof and rib control. The results show that the steel of the CMM body can change the magnetic field distribution and also alter electrical parameters of a PDS by changing its generator current. The study also shows that, depending on the distance between the wire mesh and a generator, the magnetic field can also be altered.

INTRODUCTION

Continuous mining machines (CMMs) can be up to 10 m (33') in length and more than 3 m (10') in width. These machines perform the coal cutting operations in underground room-and-pillar coal mines. Accidents during CMM operation accounts for an average of 250 injuries every year, and 43 miners have been killed by striking or pinning accidents involving CMMs in the United States from 1984 to 2015.

Because of these fatalities and injuries, the Mine Safety and Health Administration (MSHA) promulgated a regulation in 2015 that requires the use of proximity detection systems (PDSs) on all CMMs with the exception of full-face machines (Mine Safety and Health Administration, 2015). Currently, there are five different proximity detection systems that MSHA has approved as permissible for use in U.S. underground coal mines (Mine Safety and Health Administration, 2013). All of these PDSs rely on a miner-wearable component (MWC) to detect the generated magnetic fields that PDSs produce around a CMM (Schiffbauer, 2002). These systems use the magnetic field strength readings in terms of magnetic flux density from the MWC to determine whether a miner is at a safe distance from the CMM. A stable magnetic field is essential for the accuracy of a PDS.

However, it is a fact that metallic objects entering a magnetic field cause distortion and changes in that field's distribution. When a PDS is installed on a CMM, the systems are calibrated and compensation for the mass of the CMM itself is achieved. As long as no physical changes occur, the PDS provides a consistent response to the CMM operator, thus training the operator where safe and non-safe areas are relative to the CMM for advoiding striking and pinning accidents. If physical changes occur, such as changes in generator position or location, addition of a steel structure near the generator, or the presence of mine mesh for roof and rib control, the magnetic field distribution produced by the PDS will be altered. This can cause locational variance in the warning and stop zones around the CMM.

METHOD

The method used in this study makes a systematical comparison of magnetic field distributions obtained with and without the presence of a CMM and wire mesh. The magnetic field created by a generator covers a 3D spatial volume around the generator. This paper focuses on the comparison of the field distributions on a horizontal plane, and provides the data for a basic understanding of the influence of the steel body of a CMM in the presence of a mesh on the magnetic field.

Researchers from National Institute for Occupational Safety and Health (NIOSH) previously determined a shell function (in Equation 1 below) that describes the magnetic field in air around a generator with no metal mass nearby (Carr et al., 2010; Jobes et al., 2010; Li et al., 2012; Li et al., 2013a). In Equation 1, ρ denotes radial distance from the generator center to a point on the shell; a, the shape parameter, describes shape variation from a circular shell of radius b; α is the angle of the ray from the generator center to the measurement point on the shell as shown in Figure 1. A shell represents the magnetic field distribution pattern, and is a collection of points measured with a given magnetic flux density, B. For each value of B, there is a unique shell. In an environment composed of a substance, such as air, having the same permeability throughout, the greater a B is, the smaller the shell will be and the closer the shell is to the generator.

$$\rho = a\cos(2\alpha) + b \tag{1}$$

Because of the uniqueness of a shell for a given B under given conditions, the effect of a change in conditions on the magnetic field distribution can be quantitatively determined by comparing the shells for a given value of B. This paper presents a comparison of shells with and without the presence of a CMM and wire mesh.

Previously, NIOSH researchers used this method to identify the influence of coal and rock on the magnetic field distribution of proximity detection systems; it was concluded that the influence was insignificant (Li et al., 2013b). The method was also used to quantify the influence of a large steel plate on the magnetic field distribution of a proximity detection system; it was concluded that the plate had a significant influence on the magnetic field distribution (Li et al., 2017).

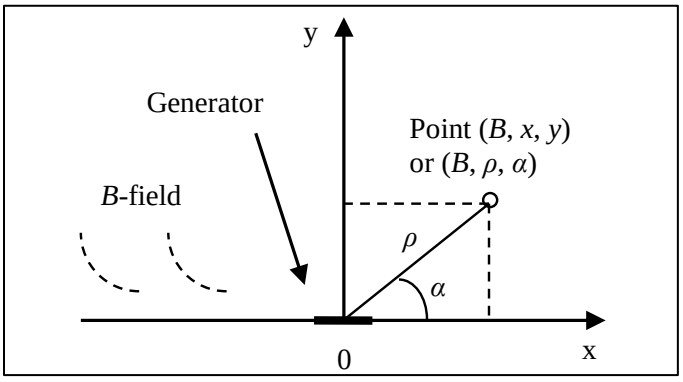

Figure 1. Point on a magnetic shell with the magnetic flux density measurement, B.

It is known that the magnetic flux density *B* is directly proportional to the current. To prevent fluctuation of *B* due to a current fluctuation caused by external environmental factors, the current to the generator is controlled to keep it the same value throughout this study.

EXPERIMENTAL RESULTS

Instrumentation

Figure 2 shows the principle block diagram of the instrumentation used in this experiment. In the diagram, the signal generator provides a 73.6-kHz signal that feeds to the RF amplifier. The amplifier provides a current sufficient to drive the generator and produce the desired magnetic field. The current flowing through the generator is measured by the current probe, and monitored with a Fluke 125 multimeter. Not shown on the figure is an IDR-200 gaussmeter with its measurement probe.

Figure 3 shows the horizontal plane polar coordinate system and the generator position on the wooden platform used in this experiment. It also shows the 3-axial magnetic probe of the IDR-200. The meter provides a vector-sum magnetic flux density reading in milliGauss (mG) at any giving point on the coordinate system.

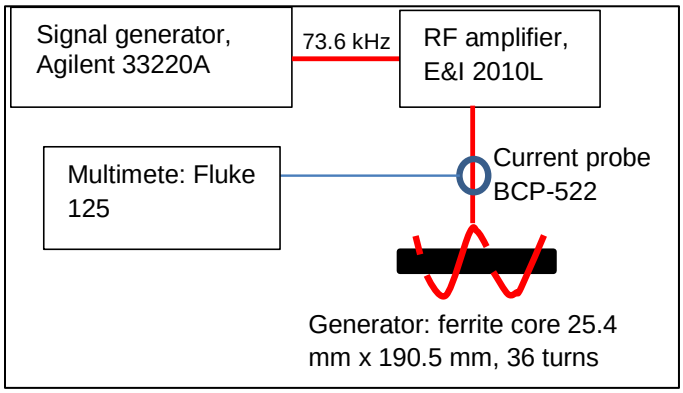

Figure 2. Instrumentations for magnetic field generation.

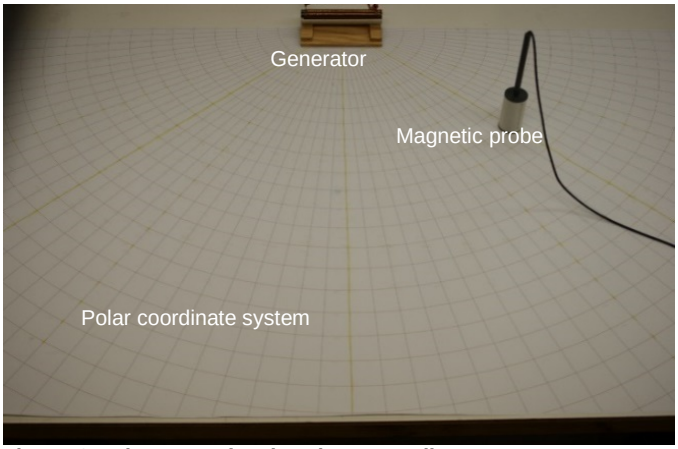

Figure 3. The setup for the plane coordinate system, generator and magnetic probe.

The same instrumentation was used for all of the experiments in this study. Several hundreds of points were measured in different locations to obtain a field distribution covering an area of 0.9 m x 2.4 m.

Experimental setups

There were three setups in this study: in the first, the system was positioned with no metal body nearby; the second setup positioned the system close to a CMM with no wire mesh present (Figure 4); and the third setup positioned the system between the CMM and a wire mesh wall in a simulated coal mine entry (Figure 5). The first setup produced a baseline field distribution with no external metallic influences. The second setup produced a field with the influence of a CMM only. The third setup produced a field with the influence of both the CMM and wire mesh.

In both the second and third setups, a 6 cm (2.4") gap was set between the generator and the body of the CMM. The wire mesh is a 15.24 cm (6") square pattern of 4-mm (0.162") steel wire. The dimensions of the simulated mesh entry are 12.2 m x 5.5 m x 3 m (40' x 18' x 10'). The mesh covers the roof and both ribs.

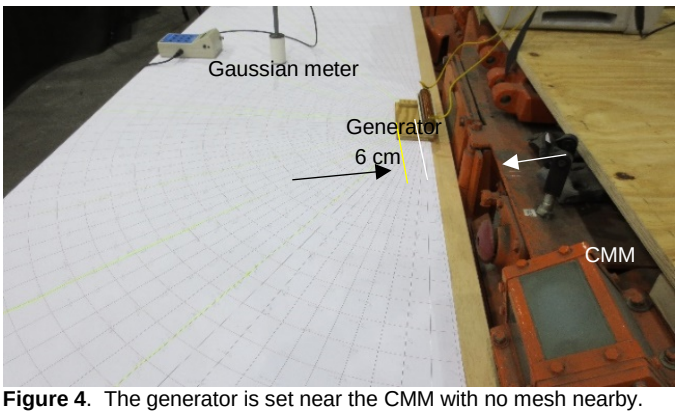

Figure 4. The generator is set near the CMM with no mesh nearby.

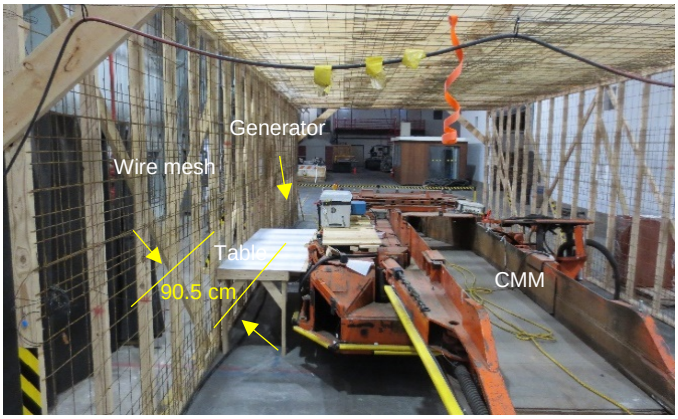

Figure 5. The experimental system positioned between the CMM and the wire mesh rib.

The influence of the CMM, in the absence of mesh on the magnetic field is illustrated with two sets of half shells in Figure 6, corresponding to magnetic flux densities of 340 mG and 6.5 mG both with and without the CMM present.

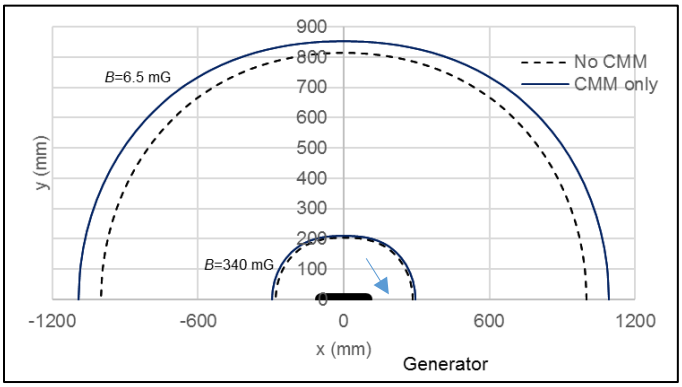

Figure 6. Comparison of magnetic field shells with and without the presence of the CMM.

Figure 6 clearly shows an enlargement of the shells when the generator was close to the CMM, indicating an enhancement of the field by the CMM steel body. It also shows that the farther the measurement is made from the generator (or the smaller the *B* value), the greater the enhancement appears. This is due to the fact that the

magnetic field distribution is highly nonlinear with distance from the generator.

This is, however, not always the case when a wire mesh is introduced into the field. The influence of the mesh on the magnetic field is illustrated in Figures 7 and 8.

Figure 7 shows two sets of magnetic field distribution shells near the CMM in the space between the CMM and the mesh. The smaller set of three shells was obtained with a measurement *B* of 275 mG and the large set of three shells with 21 mG. Measurements were taken within an area between the generator and two third of the way to the mesh. Within this area, there was no discernible influence of the mesh as compared to the influence of the CMM along. This suggests that any enhancement of the field due to the mesh is minor in this area.

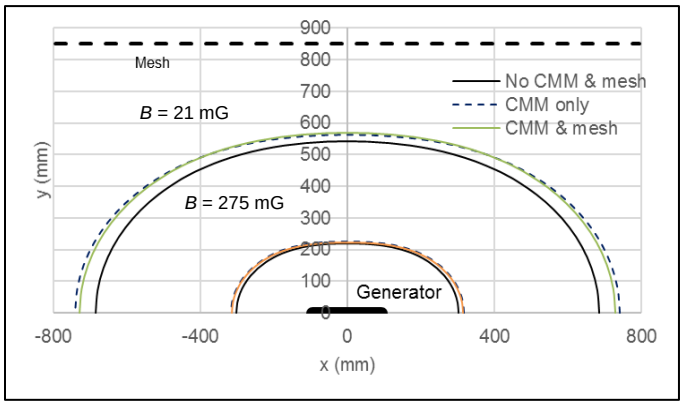

Figure 7. Part of magnetic field distribution close to the CMM. The straight dash line on the top represents the wire mesh. The position of the mesh wall as it relates to the generator is also illustrated.

Figure 8 provides one shell of the field distribution when a measurement is closer to the mesh. The figure shows the difference between the actual field measurements of *B* = 8.8 mG, indicated by diamond markers, and the model prediction in a solid curve. The measurements clearly show a departure from the model when taken closer to the mesh. The measurements show that the magnetic flux density can increase rather than decrease as the measurement approaches very closely to the mesh. This suggests that the mesh gradually strengthens its influence within 20 cm (approximately 8”), and starts to significantly distort the field near it when closer than 15 cm (approximately 6”) to the wire mesh.

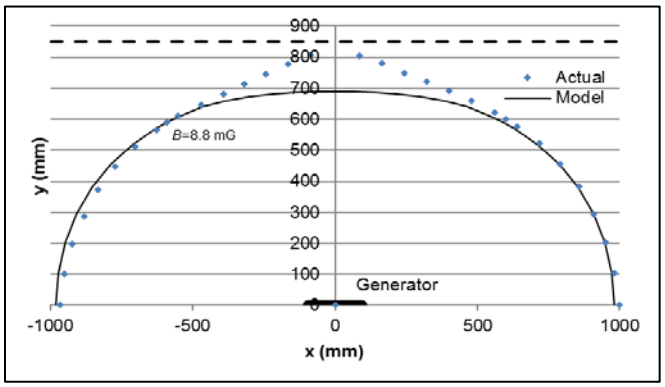

Figure 8. Comparison of the measured and modeled magnetic fields between the CMM and the mesh.

The steel of the CMM body and wire mesh can not only change the magnetic field nearby, but also alter the electrical parameters of the generator as shown in Table 1. This is due to the fact that steel is one type of electrical conductor which can serve as a load on the generator and modify the measured electrical parameters. A change of these parameters will lead to a change of generator impedance, resulting in a generator current change and field flux density change if not compensated. Consequently, a location calculated based on a magnetic density measurement can be affected.

Table 1. Measured generator electrical parameters at f = 73.6 kHz (*L*: Inductance, *R*: Resistance, *Q*: Quality factor).

Generator electrical parameters	No metal mass nearby	6 cm from CMM	Between CMM and mesh
L (μH)	174.18	165.21	164.06
R (Ω)	0.4449	1.256	1.094
Q	181.06	60.62	69.32

LIMITATIONS

This study was limited to one laboratory experimental environment, and the measurements were conducted within a small area. Additional work may be required in order to acquire more measurements for an analysis of the influence of CMM and mesh on an extended space or/and different environment. The method and measurement results presented in this paper can serve as a reference for the future study. The following items can be considered for future work.

This paper presents measurements for the magnetic field distributions with and without the presence of a CMM and/or wire mesh on a plane perpendicular to one side of the vertical surfaces of the CMM. The method can be adapted to any other angles. The results may be different depending on the particular angle used.

The measurements given in Figure 6 show that the CMM strengthens the magnetic field in the open space in front of the generator. The field distribution behind the CMM can be different from that in front because of a shielding effect caused by the steel body of the CMM. The measurements and models in the open space in front may not apply to that behind the CMM. The field behind the CMM needs to be modeled with the separate measurements.

The enhancement of the magnetic field in front of the generator can be different on a machine different from a CMM because of its size and differences in steel electromagnetic properties. The magnetic field needs to be modeled with the measurements for a given machine. The measurements, and the model presented in this paper can serve as a reference, and the method can be adapted for such a study.

As shown in Figure 8, the wire mesh can have a stronger influence at a closer proximity. This suggests that the mesh can have a significant influence on the magnetic field far from the generator and close to the mesh. This also suggests that the influence of the mesh can cover a much greater space beyond the area covered in this study because of the large volume of the mesh compared to that of the generator. The wire mesh can help the magnetic energy propagate along it for a greater distance than the magnetic field produced by the generator alone.

The modifications of the electrical parameters under influence of the steel body of the CMM and mesh can lead to a magnetic field change. A field change can, in turn, alter the position calculated from the field measurements. An automated current control system could be used to stabilize the generator current against electrical parameter changes. The automated control system can also be incorporated with other technologies to better handle the influence of wire mesh and other disturbing factors to improve the system performance of a proximity detection system given proper approval and testing.

CONCLUSIONS

This paper presents a study of the influence of the steel body of a CMM and of wire mesh on magnetic field from a proximity detection system. The mesh was installed on the roof and both ribs in a simulated coal mine entry. The study’s measurements show that the steel body of the CMM can enhance the magnetic field in the open space in front of the PDS generator. The mesh can also enhance the field in the space close to it. The closer to the mesh and the farther from the generator, the greater the enhancement. The measurements also show that the steel body of the CMM and the mesh can alter the

electrical parameters of the generator. Understanding their influence on a proximity detection system can lead to improved design and accuracy of PDSs by minimizing adverse influences. An accurate PDS can make a CMM safer to operate, which in turn will increase miners safety.

ACKNOWLEDGMENTS

The authors sincerely thank NIOSH technician, Mr. Jeffrey A. Yonkey. The authors are also thankful to NIOSH mechanical engineer, Mr. Peter Bissert, for his support and help in setting up the experimental system, and Mr. Jacob Carr, team leader of the Machine Safety Team in NIOSH, and Mr. Adam Smith, deputy director of Pittsburgh Mining Research Division in NIOSH for their comments and suggestions during the course of this research.

DISCLAIMER

The findings and conclusions in this report are those of the author(s) and do not necessarily represent the views of the National Institute for Occupational Safety and Health. Reference to specific brand names does not imply endorsement by the National Institute for Occupational Safety and Health.

REFERENCES

Carr, J.L., Jobes, C.C., Li J., 2010, “Development of a method to determine operator location using electromagnetic proximity detection.” 2010 IEEE International Workshop on Robotic and Sensors Environments (ROSE). October 15-16, 2010. Phoenix, AZ.

Jobes, C.C., Carr, J.L., 2010, “Development of an Intelligent Proximity Detection System for Continuous Mining Machine,” Presentation in Proximity Warning Systems for Mining Equipment, Charleston, WV, Sept. 15, 2010, website: https://www.cdc.gov/niosh/mining/UserFiles/workshops/proximityworkshop2010/JobesCarr-NIOSH-PDWorkshop2010-508.pdf.

Li, J., Carr, J.L., Jobes, C.C., 2012, “A shell-based magnetic field model for magnetic proximity detection systems.” Safety Science. Vol. 50, Issue 3. March, 2012. pp. 463-471.

Li, J., Jobes, C.C., Carr, J.L., 2013a, “Comparison of magnetic field distribution models for a magnetic proximity detection system.” IEEE Transaction on Industry Applications, May/June 2013, 49(3), pp. 1171-1176.

Li, J., Carr, J.L., Waynert, J.A., Kovalchik, P.G., 2013b, “Environmental Impact on the Magnetic field Distribution of a Magnetic Proximity Detection System in an Underground Coal Mine,” Journal of Electromagnetic Waves and Applications, Vol. 27, No. 18, 2013, pp. 2416-2429.

Li, J., DuCarme, J., Reyes, M., Smith, A., 2017, “Investigation of Influence of a Large Steel Plate on the Magnetic Field Distribution of a Proximity Detection System,” presented at SME Annual Meeting, Denver, CO, Feb. 18 -22. 2017.

Mine Safety and Health Administration, 2013, Approval & Certification Center, Proximity Detection Systems, https://arlweb.msha.gov/TECHSUPP/ACC/lists/18Prox.pdf.

Mine Safety and Health Administration, 2015, Department of Labor, Proximity Detection Systems for Continuous Mining Machines in Underground Coal Mines. Federal Register Vol. 80, No. 10. 30 CFR Part 75, MSHA-2010-0001.

Schiffbauer, W.H., 2002, "Active Proximity Warning System for Surface and Underground Mining Applications," Mining Engineering, Dec. 01. 2002.